UCLA
UCLA Previously Published Works

Title

LXRs Regulate ER Stress and Inflammation through Dynamic Modulation of Membrane Phospholipid Composition

Permalink

https://escholarship.org/uc/item/1870g7vn

Journal

Cell Metabolism, 18(5)

ISSN

1550-4131

Authors

Rong, Xin
Albert, Carolyn J
Hong, Cynthia
et al.

Publication Date

2013-11-01

DOI

10.1016/j.cmet.2013.10.002

Peer reviewed

LXRs regulate ER stress and inflammation through dynamic modulation of membrane phospholipid composition

Xin Rong[1,2], **Carolyn J. Albert**[7], **Cynthia Hong**[1,2], **Mark A. Duerr**[7], **Brian T. Chamberlain**[5,6], **Elizabeth J. Tarling**[3], **Ayaka Ito**[1,2], **Jie Gao**[1,2], **Bo Wang**[1,2], **Peter A. Edwards**[3,4], **Michael E. Jung**[5,6], **David A. Ford**[7], and **Peter Tontonoz**[1,2]

[1]Howard Hughes Medical Institute, University of California, Los Angeles, Los Angeles, CA 90095, USA

[2]Department of Pathology and Laboratory Medicine, University of California, Los Angeles, Los Angeles, CA 90095, USA

[3]Division of Cardiology, Department of Medicine, University of California, Los Angeles, Los Angeles, CA 90095, USA

[4]Department of Biological Chemistry, University of California, Los Angeles, Los Angeles, CA 90095, USA

[5]California NanoSystems Institute, University of California, Los Angeles, Los Angeles, CA 90095, USA

[6]Department of Chemistry and Biochemistry, University of California, Los Angeles, Los Angeles, CA 90095, USA

[7]Department of Biochemistry and Molecular Biology, and Center for Cardiovascular Research, Saint Louis University, St. Louis, MO 63104, USA

Abstract

The fatty acyl composition of phospholipids determines the biophysical character of membranes and impacts the function of membrane proteins. Here we define a nuclear receptor pathway for the dynamic modulation of membrane composition in response to changes in cellular lipid metabolism. Ligand activation of LXR preferentially drives the incorporation of polyunsaturated fatty acids into phospholipids through induction of the remodeling enzyme Lpcat3. Promotion of Lpcat3 activity ameliorates ER stress induced by saturated free fatty acids *in vitro* or by obesity and hepatic lipid accumulation *in vivo*. Conversely, Lpcat3 knockdown in liver exacerbates ER stress and inflammation. Mechanistically, Lpcat3 modulates inflammation both by regulating c-Src and JNK kinase activation through changes in membrane composition and by affecting substrate availability for inflammatory mediator production. These results outline an endogenous mechanism for the preservation of membrane homeostasis during lipid stress and identify Lpcat3 as an important mediator of LXRs effects on metabolism.

Corresponding Author: Peter Tontonoz, MD, PhD, HHMI-UCLA, 675 Charles Young Dr. MRL 6-770, Los Angeles, CA 90095, ptontonoz@mednet.ucla.edu.

Introduction

Phospholipids (PLs) are important components of biological membranes and precursors of numerous signaling molecules. PL membranes compartmentalize living cells, form intracellular organelles and provide platforms for a wide variety of physiological processes, such as vesicle trafficking, signal transduction, molecular transport, and biosynthesis. PLs also act as substrates for the generation of diverse bioactive molecules involved in signal transduction, including eicosanoids, LPA and diacyl glycerol (Holzer et al., 2011; Spector and Yorek, 1985).

The fatty acyl composition of PLs determines the biophysical characteristics of membranes, including fluidity and the assembly of specific membrane subdomains (Holzer et al., 2011; Spector and Yorek, 1985). Therefore, changes in fatty acyl composition can affect the properties of proteins associated with membranes and influence the biological processes that occur on them. Modification of the fatty acyl composition of membranes influences a range of cell processes, most importantly, the activity of membrane-bound enzymes and transporters and the localization of acylated proteins in membrane subdomains (Cornelius, 2001; Fu et al., 2011; Holzer et al., 2011). For example, membrane fatty acyl composition affects the activity of the Na+/K+-ATPase and the sarcoplasmic-endoplasmic reticulum calcium ATPase-2b (*SERCA2b*) (Cornelius, 2001; Li et al., 2004). It is also known that incorporation of saturated fatty acids into plasma membrane recruits c-Src kinase to lipid raft domains and increases its activity (Holzer et al., 2011).

In mammalian cells, PLs are initially synthesized by the *de novo* pathway and subsequently undergo remodeling through fatty acyl deacylation and reacylation, a pathway referred to as the Lands cycle (Lands, 1958). As a result, saturated fatty acids are preferably linked at the sn-1 position and unsaturated fatty acids at the *sn*-2 position. This diversity and asymmetric distribution is established largely by the remodeling process, as the *de novo* PL synthesis process has little fatty acyl-CoA substrate specificity. In the liver, a major enzyme that catalyzes the formation of phosphatidylcholine (PC) from saturated lysophosphatidylcholines (LysoPC) and unsaturated fatty acyl-CoAs is lysophosphatidyl acyltransferase 3 (Lpcat3) (Hishikawa et al., 2008; Li et al., 2012; Zhao et al., 2008). Lpcat3 preferentially synthesizes PC containing unsaturated fatty acids, particularly arachidonic acid (20:4) and linoleic acid (18:2), at the *sn*-2 position.

To date, most studies of the effects of PL fatty acyl composition on biological systems have utilized *in vitro* biochemical assays, due to the difficulty of directing specific changes in membrane composition in living cells. Therefore, there is little understanding of how regulatory pathways control PL fatty acyl composition or how such regulatory pathways could dictate cell responses. It is known that increased levels of saturated fatty acids can cause ER stress, and this has been postulated to involve charges in ER membrane composition (Borradaile et al., 2006). It is also been shown that inhibition of SCD-1 or Lpcat3 activity increases membrane saturation, secondary to changes in fatty acid production (Miyazaki et al., 2000) or phospholipid remodeling (Ariyama et al., 2010), respectively. Loss of either SCD-1 or Lpcat3 activity has been shown to enhance ER stress in cultured cells (Ariyama et al., 2010). But are there regulatory pathways that modify membrane lipid composition in response to extracellular or intracellular cues? Furthermore, could such pathways be targeted pharmacologically to manipulate ER membrane composition? Finally, what is the contribution of PL remodeling to ER stress responses in the setting of metabolic disease?

The Liver X receptors (LXRs) are important regulators of cholesterol and fatty acid homeostasis and potent inhibitors of inflammation (Hong and Tontonoz, 2008). However,

the impact of LXRs on the major constituents of membranes–phospholipids–has not been rigorously investigated. Here we show that LXRs are regulators of membrane phospholipid composition and that this previously unappreciated action underlies the ability of LXRs to influence ER stress and inflammation. *Lpcat3*, which encodes a key enzyme in the PL remodeling pathway, is a direct LXR target gene in mice and humans. LXR activation promotes the incorporation of unsaturated fatty acids into PL through Lpcat3, thereby reducing hepatic ER stress and inflammation in the context of genetic obesity. These studies identify the LXR-Lpcat3 pathway as an important modulator of PL metabolism, metabolic stress responses and inflammation.

Results

Lpcat3 is a direct target of LXR in mice and humans

We previously identified *Lpcat3* (also known as MBOAT5) as an LXR-responsive gene through transcriptional profiling studies of BV-2 cells (Zelcer et al., 2007). *Lpcat3* was also reported to be responsive to synthetic LXR agonists in other cell lines (Demeure et al., 2011). However, the dependence of *Lpcat3* on the genetic expression of LXRα and LXRβ has not been examined. *Lpcat3* is widely expressed in mice, with especially prominent expression in metabolic tissues (Fig. S1A). Exposure of primary mouse hepatocytes to the synthetic LXR agonists GW3965 or T1317 induced the expression of *Lpcat3* as well as the established targets *Idol* and *Abca1* (Fig. 1A). The combination of LXR and RXR ligands further boosted *Lpcat3* expression (Fig. 1B). Importantly, the ability of LXR agonist to promote *Lpcat3* expression was lost in *Lxraβ–/–* cells. Furthermore, both LXRα and LXRβ are competent to regulate *Lpcat3*, as the response to ligands was comparable between *Lxra −/–* and *Lxrβ–/–* cells (Fig. 1B and Fig. S1B). We also observed regulation of *Lpcat3* by LXR agonists in several other cell types, including primary macrophages, RAW264.7 cells and Hep3B cells (Fig. S1C, D and G). Regulation of *Lpcat3* by LXR was not sensitive to cycloheximide, suggesting that it was a direct transcriptional effect (Fig. S1E). It was also not secondary to the induction of SREBP-1c, because oxysterols that block SREBP processing still induced *Lpcat3* expression (Fig. S1F, G). Finally, administration of GW3965 (40 mg/kg/day) for 3 days to C57Bl/6 mice induced the expression of *Lpcat3* in multiple tissues, including liver, fat, muscle and kidney (Fig. 1C and **S1H**).

Given the activity of Lpcat3, we reasoned that LXR activation might regulate PL fatty acyl composition. Using an acyltransferase assay with radiolabeled fatty acyl-CoA and LysoPL, we found that LXR agonist increased lysophosphatidylcholine acyltransferase activity and drove the formation of PC (Fig. 1D). Furthermore, ESI-MS/MS analysis of whole-cell lipid extracts showed that LXR ligand treatment markedly increased the abundance of polyunsaturated PC, especially arachidonoyl (20:4) and linoleoyl (18:2)-containing PC, in RAW 264.7 cells (Fig. 1E). The abundance of monounsaturated PC and saturated PC was not affected or even reduced (Fig. 1E). On the other hand, stable knockdown Lpcat3 expression in RAW 264.7 cells with shRNA constructs reduced Lpcat3 expression and activity (Fig. S1I), as well as the amount of 20:4 and 18:2-containing PC (Fig 1F). The regulation of PL metabolism by LXR was also evident *in vivo*. Treatment of C57BL/6 mice with GW3965 for 2 days led to a change in the abundance of several polyunsaturated PC species in total liver extracts (Fig. 1G), including those containing linoleic acid (18:2), one of the preferred substrates of Lpcat3 (Hishikawa et al., 2008).

LXR suppresses saturated fatty acid-induced endoplasmic reticulum stress

High levels of saturated fatty acids such as palmitic acid (PA) are postulated to trigger ER stress pathway by altering membrane dynamics and integrity (Borradaile et al., 2006). The observation that LXR increased levels of unsaturated PLs led us to explore whether LXR

was able to protect cells from saturated fatty acid-induced ER stress. We first assessed the unfolded protein response (UPR)–signaling pathways activated by the accumulation of unfolded proteins commonly used as indicators of ER stress. Pretreatment of Hep3B hepatoma cells with GW3965 blunted the induction of the downstream UPR target genes CHOP and ATF3 by PA in a dose-dependent manner (Fig. 2A and **S2A**). Similar effects were observed in primary mouse hepatocytes and macrophages (Fig. S2B, C). Interestingly, however, LXR ligand had no effect on the induction of ER stress by thapsigargin (Fig. 2A), suggesting that LXR specifically modulates lipid-induced ER stress. The protective effects of LXR agonist were observed in wild-type but not in *Lxraβ*–/– primary hepatocytes, indicating that they are indeed mediated by LXRs (Fig. 2B). The absence of LXRs also sensitized hepatocytes to PA-induced ER stress markers. In addition, LXR agonist treatment decreased the formation of spliced *Xbp1* mRNA and reduced the phosphorylation of PERK and EIF2α (Fig. 2C, D).

The accumulation of excess free cholesterol in macrophages is also known to trigger the activation of ER stress pathways (Feng et al., 2003). Treatment of primary mouse macrophages with LXR agonist blunted the induction of UPR target genes induced by loading with acetylated LDL in the presence of an ACAT inhibitor (Fig. 2E). Chronic ER stress induced by lipotoxicity eventually causes cell apoptosis. Hep3B cells pretreated with LXR ligand were protected from saturated fatty acid-induced apoptosis as assessed by caspase-3 activity (Fig. S2D, E).

Lpcat3 contributes to LXR-dependent suppression of ER stress signaling

Next we addressed the mechanism by which LXR protects cells from lipid-induced ER stress. Prior biochemical studies have shown that unsaturated PLs increase membrane dynamics, an effect that might potentially reverse deleterious effects of saturated fatty acids on membrane structure. We therefore hypothesized that LXRs might reduce ER stress by increasing the proportion of polyunsaturated PLs in membranes through *Lpcat3* induction. Consistent with the observation that knockdown of *Lpcat3* decreased membrane PL unsaturation (Fig. 1F), loss of Lpcat3 also affected fatty acid-induced ER stress. siRNA-mediated knockdown of *Lpcat3* in Hep3B cells markedly enhanced the expression of CHOP and ATF3 (Fig. 2F), as well as the phosphorylation of eIF2a in response to PA (Fig. 2G).

To address whether Lpcat3 activity mediated protective effects of LXR on ER stress, we treated primary hepatocytes with LXR agonist in the presence or absence of Lpcat3 knockdown. LXR agonist strongly suppressed the expression of sXBP-1, ATF3 and ATF-4 in response to PA (Fig. 3A). The magnitude of suppression by LXR agonist was reduced but not abolished by shRNA-mediated knockdown of Lpcat3. The residual effect of LXR agonist on ER stress is consistent with prior studies showing that SCD-1 also inhibits ER stress (Erbay et al., 2009).

To establish that the effects of LXR on cellular PL composition were dependent on Lpcat3, we examined primary mouse hepatocytes deficient in either LXR or Lpcat3 expression. Treatment of wild-type hepatocytes with GW3965 increased the abundance of PC species containing 20:4 or 18:2 acyl chains, and this effect was completely abrogated in hepatocytes from mice lacking both LXRα and LXRβ (DKO; Fig. 3B). Furthermore, shRNA-mediated knockdown of *Lpcat3* expression in primary hepatocytes blunted the ability of LXR agonist to induce levels of these same unsaturated PC species (Fig. 3C). Thus, the ability of GW3965 to modulate cellular PL composition is dependent on both LXR and Lpcat3 expression.

The primary function of Lpcat3 is to catalyze the formation of polyunsaturated PL. Therefore, we reasoned that polyunsaturated PLs produced by Lpcat3 are the bioactive

molecules that mediate the effects of the LXR pathway on ER stress. If this hypothesis is correct, then treatment of cells with arachidonoyl-containing PC should mimic the protective effects. Indeed, pretreatment of cells with liposomes made with 16:0, 20:4 PC, but not saturated 16:0, 18:0 PC, inhibited PA-induced ER stress in a dose-dependent manner (Fig. 3D). Since polyunsaturated fatty acids are known to reduce ER stress, we considered the possibility that the protective effects of arachidonoyl-containing PC were secondary to the enzymatic release of arachidonic acid from the PC. To rule out this possibility, we used the phospholipase A2 inhibitor bromoenol lactone (BEL), to prevent the release of arachidonic acid. 16:0, 20:4 PC retained its protective effects even in the presence of BEL treatment (Fig. 3E), strongly suggesting that the arachidonoyl-containing PC itself is the active molecule. In sum, these results demonstrate that LXR activation protects cells from lipid-induced ER stress, at least in part, by promoting the Lpcat3-mediated formation of unsaturated PC species.

The LXR-Lpcat3 pathway regulates metabolic ER stress in vivo

ER stress has been observed in a number of metabolic diseases and is postulated to be a key pathogenic factor in their development. Therefore, we investigated the physiological impact of the LXR-Lpcat3 pathway on ER stress in mouse models of metabolic disease. To test whether endogenous LXR signaling influenced the development of hepatic ER stress induced by lipid-rich diet, we fed *Lxraβ*–/– (DKO) mice and wild-type littermates a Western diet for 12 weeks. DKO mice exhibited increased expression of ER stress markers, including ATF3 and CHOP (Fig. 4A). Furthermore, increased ER stress pathway activation correlated with reduced *Lpcat3* expression in the livers of DKO mice (Fig. 4A). To address whether *Lpcat3* deficiency would exacerbate metabolic ER stress *in vivo*, we used adenoviral vectors to deliver an shRNA construct targeting *Lpcat3* to the livers of *ob/ob* mice–a genetic model of obesity known to exhibit hepatic ER stress (Ozcan et al., 2004). shRNA-mediated knockdown of Lpcat3 induced the expression of a panel of genes linked to ER stress (sXBP1, CHOP, ATF3, BIP; Fig. 4B) compared to shRNA control. This was also accompanied by increased phosphorylation of PERK and eIF2a (Fig. 4C), consistent with enhanced ER stress pathway activation.

Since the ability of Lpcat3 to ameliorate ER stress *in vitro* correlated with production of unsaturated PC (Figs. 1 and 2), we analyzed the effect of Lpcat3 expression on PL fatty acyl composition *in vivo*. ESI-MS/MS analysis of total lipids revealed clear changes in PC fatty acyl composition in mouse liver transduced with shLpcat3 adenovirus compared to control, and these changes were largely consistent with our results in cultured cells. The amount of arachidonoyl- and linoloyl-containing PC species was reduced by shRNA-mediated knockdown of Lpcat3, while the amounts of saturated or mono-unsaturated PC were not changed or even increased by Lpcat3 knockdown (Fig. 4D). Similar trends were observed for PE fatty acyl composition, in line with prior reports that PE is also a substrate for Lpcat3-dependent remodeling (Fig. S3A).

After 7 days of transduction with shLpcat3, *ob/ob* mice exhibited a modest decrease in blood glucose levels and no significant change in plasma insulin, suggesting that there was minimal effect on the insulin resistance phenotype over this time frame (Fig. S3B). Plasma TG levels were modestly increased and liver TG levels were decreased (Fig. S3B). These observations are consistent with prior reports that Lpcat3 and ER stress affect VLDL secretion from the liver (Li et al., 2012; Wang et al., 2012).

We transduced adenoviral vectors expressing EGFP control or Lpcat3 into *ob/ob* mice to ask whether increased Lpcat3 activity in the liver might ameliorate lipid-induced ER stress. Adenoviral expression of Lpcat3 in *ob/ob* livers reduced expression of ATF3 and there was a trend towards decreased spliced XBP-1 (Fig. 5A). Interestingly, Lpcat3 expression in this

model was also associated with an improvement in glucose homeostasis. Mice expressing Lpcat3 had reduced blood glucose levels, plasma insulin levels, and insulin resistance index compared to control-transduced mice (Fig. 5B). There was no difference in liver or plasma TG levels or plasma free fatty acids. Lpcat3-transduced *ob/ob* mice also showed modest improvement in glucose tolerance compared to controls (Fig. 5C).

We employed *db/db* mice as an additional model of lipid-induced hepatic ER stress. These mice exhibit more severe insulin resistance, hepatic steatosis and inflammation compared to *ob/ob* mice. Expression of Lpcat3 in *db/db* mice reduced the expression of ER stress-associated genes, including CHOP, ATF3 and sXBP-1 (Fig. 5D). Collectively, these data implicate the LXR-Lpcat3 pathway as a physiological regulator of PL fatty acyl composition in mouse liver that affects hepatic UPR signaling in the setting of metabolic stress. Although we observed relatively modest changes in lipid and glucose metabolism in response to Lpcat3-dependent perturbations in ER stress over the 7-day time frame of these studies, we cannot exclude the possibility that more chronic changes in Lpcat3 activity might have more robust metabolic effects.

Lpcat3 activity modulates inflammatory responses in vivo

Since alteration of membrane lipid composition has been shown to affect inflammatory signaling, we further investigated the influence of Lpcat3 activity on hepatic inflammation. Histological analysis of livers from wild-type C57BL/6 mice transduced with shLpcat3 adenovirus revealed marked infiltration of F4/80+ macrophages, consistent with ongoing inflammation (Fig. 6A). Macrophage infiltration in Lpcat3-knockdown livers was confirmed by analysis of F4/80 gene expression (Fig. S4A). Furthermore, expression of pro-inflammatory cytokines (MCP-1, TNFα and IL-1β) was elevated in shLpcat3-transduced livers compared to controls, indicative of enhanced inflammatory signaling (Fig. S4B). To comprehensively analyze the impact of Lpcat3 knockdown on hepatic gene expression, we performed transcriptional profiling. This analysis revealed that a large number of pro-inflammatory genes were induced in response to Lpcat3 knockdown, including pro-inflammatory cytokines and chemokines, cytokine and chemokine receptors, and complement components (Fig. 6B).

Next, we investigated whether Lpcat3 activity could also modulate hepatic inflammatory responses in the setting of metabolic disease and hepatic steatosis. Indeed, knockdown of Lpcat3 expression with an adenoviral shRNA vector in *ob/ob* mouse liver exacerbated the expression of a panel of pro-inflammatory cytokines and chemokines, including Cox-2, MCP-1, and MIP-2 (Fig. 6C). Consistent with increased hepatic inflammation, plasma ALT and AST levels were also increased (Fig. S4C).

We further tested the effect of increased Lpcat3 activity on hepatic inflammatory signaling in both wild-type and genetically obese mice. Adenovirus-mediated Lpcat3 expression in wild-type livers reduced the basal expression of a panel of inflammatory cytokines (Fig. 6D). In fact, many of the same genes increased by Lpcat3 knockdown were reduced by Lpcat3 expression. Interestingly, we did not observe any difference in ER stress markers in wild-type mice overexpressing Lpcat3 (Fig. S4D), suggesting that the effects of Lpcat3 on inflammation may be independent of ER stress. We also employed *ob/ob* mice as a model of lipid-induced hepatic inflammation. Remarkably, expression of Lpcat3 in livers of these mice ameliorated inflammation, evidenced by a marked reduction in the expression of inflammatory chemokines and cytokines (Fig. 6E). Similar results on inflammatory markers and plasma AST and ALT levels were also observed in *db/db* mice (Fig. S4E, F). These data suggest that Lpcat3 is a regulator of hepatic inflammation and that enhanced Lpcat3 activity has beneficial effects on inflammation in the setting of metabolic disease.

Lpcat3 activity affects the production of lipid inflammatory mediators

To address whether the effects of Lpcat3 activity on inflammation were cell-autonomous, we analyzed inflammatory signaling in cultured primary hepatocytes and macrophages. shRNA-mediated knockdown of Lpcat3 in primary mouse hepatocytes with an adenoviral vector led to increased expression of well-established hepatic inflammatory mediators, including CXCL10 and MIP-2 (Fig. 7A). Furthermore, knockdown of Lpcat3 ameliorated the suppressive effect of LXR agonist on the expression of these genes. Similarly, siRNA-mediated knockdown of Lpcat3 expression in murine peritoneal macrophages augmented the induction of inflammatory genes in response to LPS (Fig. S5A). Lpcat3 knockdown in macrophages blunted the ability of LXR agonist to repress MCP-1, and to a lesser extent, TNF-α expression. This observation suggests that Lpcat3 induction by LXR may contribute to the repressive effects of LXR agonists on some inflammatory genes.

Products of arachidonic acid and lysoPCs are well-known pro-inflammatory lipid mediators (Funk, 2001; Kabarowski, 2009). Since activation of LXR-Lpcat3 pathway converts the bioactive free arachidonic acid and lysoPCs into PLs, we hypothesized that increased activity of this pathway may limit inflammatory mediator production by limiting substrate availability. In support of this idea, acute induction of Lpcat3 activity by treatment with LXR agonist (GW3965) strongly reduced the levels of multiple LysoPC species (Fig. 7B). This effect was completely abolished by Lpcat3 knockdown. Although we did not observe changes in lysoPC levels between shCtrl- and shLpcat3-treated WT mice after 8 d, this may reflect compensatory responses in LysoPC metabolism in the setting of chronic alteration of Lpcat3 activity. Furthermore, GC-MS analysis revealed greatly increased levels of free arachidonic acid in livers of wild-type mice in which Lpcat3 expression was knocked down (Fig. 7C). Conversely, ectopic expression of Lpcat3 in livers of wild-type mice markedly decreased levels of free arachidonate (Fig. 7D). We also analyzed PGE2 production by LPS-stimulated macrophages *in vitro*. Consistent with our hypothesis that Lpcat3 activity limits arachidonic acid availability for eicosanoid synthesis, ligand activation of LXR in these cells repressed PGE$_2$ secretion (Fig. S5B). Collectively, these findings suggest that Lpcat3 activity affects inflammation, at least in part, through modulation of lipid inflammatory mediator production.

Lpcat3 activity modulates c-Src activation in membrane microdomains

Increasing membrane saturation has been shown to affect the compartmentalization and activity of membrane-bound c-Src kinase by recruiting the protein to membrane microdomains, sometimes referred to as lipid rafts (Holzer et al., 2011). Activated c-Src initiates the downstream JNK signaling pathway, a central regulator of inflammation (Wellen and Hotamisligil, 2005). Given that activation of Lpcat3 reduces membrane saturation, we hypothesized that the LXR-Lpcat3 pathway might regulate the activity of the c-Src-JNK pathway through modulation of membrane lipid composition. In support of this idea, treatment of primary macrophages with LXR agonist decreased LPS-stimulated phosphorylation of membrane-bound c-Src kinase (Fig. 7E). Induction of ABCA1 served as a positive control for LXR activation. On the contrary, knockdown of Lpcat3 expression with an adenoviral shRNA vector in *ob/ob* mouse liver increased the phosphorylation of c-Src and JNK (Fig. 7F). To examine whether Lpcat3 activity altered the compartmentalization and activation of c-Src in membranes microdomains, Hep3B cells were treated with Lpcat3 siRNA followed by PA stimulation. Detergent-resistant membrane (DRM) was isolated through density gradient centrifugation. DRM and its associated proteins were enriched in fraction 2, as indicated by Flot1; while soluble protein and cell debris were enriched in fraction 3 and 4, as shown by TfR, a membrane protein excluded from DRM. In Lpcat3-knockdown cells, phospho-c-Src abundance was greatly increased in the DRM fraction, although the amount of total c-Src protein in DRM was unchanged (Fig.

7G). This observation strongly suggests that a reduction in the abundance of Lpcat3 PL products alters the structure of membrane microdomains in a way that favors the activation of c-Src. Thus, in addition to modulation of lipid inflammatory mediators, Lpcat3 activity also regulates the activation of the c-Src-JNK pathway. Collectively, our results define mechanisms whereby LXR signaling modulates ER and inflammatory homeostasis in response to changing cellular lipid levels through Lpcat3.

Discussion

Given the difficulty of manipulating fatty acyl composition in living cells, few studies have addressed the physiological impact of dynamic changes in PL fatty acyl composition. We have shown here that LXR regulates PL fatty acyl composition through regulation of Lpcat3. Induction of Lpcat3 by LXR promotes the formation of polyunsaturated PLs and decreases membrane saturation. This membrane remodeling counteracts saturated fatty acid-induced ER stress in hepatocytes and mouse liver. Furthermore, the LXR-Lpcat3 pathway ameliorates hepatic inflammation by modulating c-Src kinase activation and controlling the availability of lipid inflammatory mediators. These observations identify Lpcat3 regulation as an important mechanism by which LXR signaling modulates lipid homeostasis in both physiology and disease.

Studies of *in vitro* biochemical systems have demonstrated that changes in PL fatty acyl composition strongly affect membrane protein function. Whether membrane fatty acyl composition is actively regulated by endogenous signaling pathways has not been intensively studied. The SREBP pathway is an important determinant of membrane lipid composition due to its regulation of cholesterol and PL synthesis (Brown and Goldstein, 1999). Our study has identified the LXR-Lpcat3 pathway as a physiological regulator of membrane fatty acyl composition. This function fits well with LXRs' previously defined roles as coordinators of cholesterol and fatty acid metabolism. The fatty acyl chain of polyunsaturated PL assumes a flexible and bent conformation, resulting in decreased membrane order and increased membrane fluidity. Notably, cellular levels of cholesterol, another important cellular membrane structural component, are also regulated by LXR signaling. Activation of LXRs reduces cholesterol levels by promoting cholesterol efflux and inhibiting cholesterol uptake (Calkin and Tontonoz, 2012), an effect that would be expected to impact membrane order and fluidity. LXR is also an important regulator of SCD-1 expression (Chu et al., 2006; Repa et al., 2000). Increased desaturation of newly synthesized fatty acids increases substrate availability for synthesis of unsaturated PC. Indeed, increased SCD-1 expression has been proposed to alleviate ER stress in atherosclerosis (Erbay et al., 2009). Thus, LXR signaling alters membrane lipid composition and modifies membrane physical properties through multiple mechanisms.

ER stress is observed in livers of obese mice and humans and has been postulated to be a contributor to metabolic disease. We observed modest changes in systemic metabolism in response to short-term alterations in Lpcat3 activity. In particular, adenoviral expression of Lpcat3 in the livers of *ob/ob* mice lowered blood glucose and insulin levels. However, more chronic models (e.g. transgenics or knockouts) are likely better suited to test the ability of Lpcat3 to affect the development or progression of metabolic disease.

The exact mechanisms by which obesity activates ER stress are incompletely understood, but saturated free fatty acids are believed to alter ER membrane structure (Borradaile et al., 2006; Volmer et al., 2013). Excess saturated fatty acids are rapidly incorporated into PLs in ER membranes, resulting in increased membrane order and reduced membrane fluidity. Although the nature of the link between membrane fluidity and ER stress is not yet clear, a growing body of evidence suggests that altered lipid composition affects the function of ER

membrane proteins. For instance, enrichment of ER membrane with saturated PLs *in vitro* inhibits the activity of the calcium pump SERCA2b (Li et al., 2004), leading to ER Ca^{2+} depletion and the activation of ER stress. Recently, increased ER membrane saturation has been shown to enhance the activation of IRE1α and PERK directly (Volmer et al., 2013). Our results support a biophysical model in which the LXR-Lpcat3 pathway alters membrane fatty acyl composition and fluidity, thereby counteracting the membrane-toxic effects of saturated fatty acid and alleviating ER stress.

Activated LXRs strongly suppress the expression of pro-inflammatory cytokines and chemokines in response to inflammatory stimuli (Hong and Tontonoz, 2008). However, the precise mechanisms underlying LXR's anti-inflammatory effects are not clear. In this study, we have shown that *Lpcat3*, a direct transcriptional target of LXR, strongly modulates inflammatory responses *in vitro* and *in vivo*. Knockdown of *Lpcat3* in mouse liver induced a series of inflammatory responses, including macrophage infiltration, increased serum ASL and ALT, and upregulation of pro-inflammatory cytokines and chemokines. Conversely, overexpression of Lpcat3 had opposite effects, indicating that Lpcat3 enzyme activity is a potent modifier of inflammatory responses.

How does Lpcat3-mediated modulation of PL composition influence inflammatory responses in hepatocytes? JNK is a pro-inflammatory kinase whose downstream signaling cascade controls various inflammatory responses (Solinas et al., 2007; Tuncman et al., 2006). Recently, Holzer *et al.* reported that changes in membrane lipid composition affect JNK activation by altering the compartmentalization and activation of c-Src kinase in cell membranes (Holzer et al., 2011). Treatment of cells with PA increases the partitioning and activation of c-Src in membrane subdomains with higher order and rigidity, which in turn phosphorylates JNK and initiates the JNK signaling cascade. We found that knockdown of Lpcat3, which reduces membrane fluidity, also increased the activation of c-Src and JNK in livers of obese mice. Moreover, knockdown of Lpcat3 in hepatocytes enhanced the activation of c-Src in DRMs in response to PA stimulation, directly implicating c-Src and JNK signaling in the inflammatory effects of Lpcat3. These data suggest that modulation of membrane lipid composition is a key mechanism by which Lpcat3 activity affects inflammatory signaling in hepatocytes.

In addition to affecting membrane physical properties, modulation of Lpcat3 activity alters the availability of the two substrates in the enzymatic reaction, LysoPC and free arachidonic acid, both of which have been demonstrated to be involved in inflammatory responses. The reduction in LysoPC and arachidonic acid availability may be an additional mechanism by which Lpcat3 activity influences inflammatory signaling. However, further studies are needed to elucidate the precise signaling pathways that connect LysoPC and arachidonic acid with hepatic inflammatory responses. Recently, another study reported that the LXR-Lpcat3 pathway also regulates PL metabolism in human primary macrophages (Ishibashi et al., 2013). But in contrast to our work, that study suggested that LXR ligands stimulate eicosanoid secretion and pro-inflammatory effects. Such effects are difficult to reconcile with the large body of literature supporting the net anti-inflammatory actions of endogenous LXR signaling *in vitro* and *in vivo* (Hong and Tontonoz, 2008). We find LXR signaling to be strongly anti-inflammatory in macrophages, although synthetic LXR agonists can exert non-specific inflammatory effects in some contexts.

Abnormal cellular membrane lipid composition and fluidity have been observed in several metabolic diseases. For example, cellular membranes from atherosclerotic and obese individuals show decreased fluidity (Faloia et al., 1999). Although direct *in vivo* evidence is still needed to establish the pathogenic effects of abnormal membrane lipid composition, multiple *in vitro* studies have demonstrated that alterations in membrane lipid composition

affect cellular ion balance, inflammation, and ER stress, all of which are involved in the development of chronic metabolic diseases. Our data indicate that increased Lpcat3 activity is able to modulate membrane lipid composition, multiple *in vitro* studies have demonstrated that alterations in membrane lipid composition affect cellular ion balance, inflammation, and ER stress, all of which are involved in the development of chronic metabolic diseases. Our data indicate that increased Lpcat3 activity is able to modulate membrane lipid composition, increase membrane fluidity, and most importantly, reduce inflammation and ER stress in liver. These findings suggest that regulation of PL remodeling might represent a novel strategy for intervention in chronic metabolic diseases.

Experimental Procedures

Reagents and Plasmids

LXR ligands GW3965 and T0901317 were synthesized according to published methods (Collins et al., 2002a; Collins et al., 2002b; Li et al., 2000). Thapsigargin and oxysterols were from Sigma (St. Louis, MO). Sequences of shRNA targeting mouse Lpcat3 were designed using BLOCK-iT RNAi designer tool (Invitrogen). Sense and antisense oligos were annealed and cloned into pENTR/U6 vector using the BLOCK-iT U6 RNAi Entry Vector Kit (Invitrogen). The shRNA constructs were further cloned into a gateway adapted pBabe-puro plasmids through LR recombination (Invitrogen). The following shRNA oligos were used: lacZ shRNA CACCGGGCCAGCTGTATAGACATCTCGAA AGATGTCTATACAGCTGGCCC; Lpcat3 shRNA CACCGCAGGTCAGCAGTCTAATTCGTTCAAGAGACGAATTAGACTGCTGACC TGC. Only sense strands are shown. Ad-Lpcat3 and Ad-shLpcat3 adenoviral vectors were generated by LR recombination of pEntr-Lpcat3 or pEntr/U6-shLpcat3 and pAd/CMV/V5-DEST (Invitrogen). Viruses were amplified, purified and titred by Viraquest Inc.

Cell Culture

HEK293T, HEK293A, Huh7, and Raw264.7 cells were cultured in DMEM with 10% fetal bovine serum (FBS) and antibiotics at 37°C and 5% CO2. Hep3B cells were cultured in EMEM. Mouse primary hepatocytes were isolated from 2- to 3-month-old male C57BL/6 mice, *Lxrα⁻/⁻, Lxrβ⁻/⁻* or *Lxrαβ⁻/⁻* mice as described in (Pei et al., 2006) and cultured in William E medium with 5% FBS. Bone marrow-derived macrophages and thioglycollate-elicited or concanavalin A-elicited peritoneal macrophages were isolated as described (Castrillo et al., 2003; Feng et al., 2003). Raw 264.7 stable cell lines were made by pBabe retro-viral vectors as described (Venkateswaran et al., 2000).

Gene Expression and Microarray Analysis

Total RNA was isolated with Trizol (Invitrogen). cDNA was synthesized with the iScript cDNA synthesis kit (Bio-Rad, Hercules, CA) and quantified by real-time PCR using SYBR Green (Diagenode, Denville, NJ) on an ABI 7900 instrument. Gene expression levels were determined by using a standard curve. Each gene was normalized to 36B4 or GAPDH. Primer sequences are available upon request. For microarray experiments, liver tissues were harvested 8 d post adenovirus injection. RNA was pooled from n 5 biological replicates and processed in the UCLA Microarray Core Facility using Gene-Chip Mouse Gene 430.2 Arrays (Affymetrix, Santa Clara, CA). Data analysis was performed using software GenespringGX (Agilent, Santa Clara, CA).

Animal Studies

8–12 week old male C57BL/6, *ob/ob*, and *db/db* mice were acquired from Jackson Laboratory (Sacramento, CA). *Lxrα⁻/⁻, Lxrβ⁻/⁻* and *Lxrαβ⁻/⁻* mice were originally from

David Mangelsdorf. Mice were fed a standard chow diet and housed in a temperature-controlled environment under a 12-h light-dark cycle under pathogen-free conditions. For adenoviral infections, 8–10 week old male mice were injected with 2 x 10^9 or 3 x 10^9 PFU by tail-vein. Mice were sacrificed 7–9 d later following a 6 h fast. Fasting blood glucose was measured before sacrifice. Liver tissues were collected and immediately frozen in liquid nitrogen and stored at −80°C or fixed in 10% formalin. Blood was collected by direct cardiac puncture with plasma separated by centrifugation. ALT and AST were determined at the UCLA core facility. Plasma lipids were measured using Wako L-Type TG M kit and Wako HR series NEFA-HR(2) kit (Wako, Richmond, VA). Liver triglycerides were extracted using Bligh-Dyer lipid extraction (Bligh and Dyer, 1959) and measured by Wako L-Type TG M kit (Wako, Richmond, VA). Animal experiments were conducted in accordance with the UCLA Animal Research Committee.

Statistical analysis

Statistics were performed using Student's t test (2 groups) or ANOVA (>2 groups), with post hoc tests to compare to the control group. Data are presented as means ± SEM or means ± SD as indicated and considered statistically significant at $p < 0.05$.

Supplementary Material

Refer to Web version on PubMed Central for supplementary material.

Acknowledgments

References

Ariyama H, Kono N, Matsuda S, Inoue T, Arai H. Decrease in membrane phospholipid unsaturation induces unfolded protein response. The Journal of biological chemistry. 2010; 285:22027–22035. [PubMed: 20489212]

Bligh EG, Dyer WJ. A rapid method of total lipid extraction and purification. Canadian journal of biochemistry and physiology. 1959; 37:911–917. [PubMed: 13671378]

Borradaile NM, Han X, Harp JD, Gale SE, Ory DS, Schaffer JE. Disruption of endoplasmic reticulum structure and integrity in lipotoxic cell death. Journal of lipid research. 2006; 47:2726–2737. [PubMed: 16960261]

Brown MS, Goldstein JL. A proteolytic pathway that controls the cholesterol content of membranes, cells, and blood. Proceedings of the National Academy of Sciences of the United States of America. 1999; 96:11041–11048. [PubMed: 10500120]

Calkin AC, Tontonoz P. Transcriptional integration of metabolism by the nuclear sterol-activated receptors LXR and FXR. Nature reviews. Molecular cell biology. 2012; 13:213–224. [PubMed: 22414897]

Castrillo A, Joseph SB, Vaidya SA, Haberland M, Fogelman AM, Cheng G, Tontonoz P. Crosstalk between LXR and toll-like receptor signaling mediates bacterial and viral antagonism of cholesterol metabolism. Molecular cell. 2003; 12:805–816. [PubMed: 14580333]

Chu K, Miyazaki M, Man WC, Ntambi JM. Stearoyl-coenzyme A desaturase 1 deficiency protects against hypertriglyceridemia and increases plasma high-density lipoprotein cholesterol induced by liver X receptor activation. Molecular and cellular biology. 2006; 26:6786–6798. [PubMed: 16943421]

Collins, JL.; Fivush, AM.; Maloney, PR.; Stewart, EL.; Willson, TM. Preparation of substituted phenylacetamides and benzamides as agonists for Liver X receptors (LXR). PCT Int Appl. WO 2002/024632 A2 20020328. 2002a.

Collins JL, Fivush AM, Watson MA, Galardi CM, Lewis MC, Moore LB, Parks DJ, Wilson JG, Tippin TK, Binz JG, Plunket KD, Morgan DG, Beaudet EJ, Whitney KD, Kliewer SA, Willson TM. Identification of a nonsteroidal liver X receptor agonist through parallel array synthesis of tertiary amines. Journal of medicinal chemistry. 2002b; 45:1963–1966. [PubMed: 11985463]

Cornelius F. Modulation of Na,K-ATPase and Na-ATPase activity by phospholipids and cholesterol. I. Steady-state kinetics. Biochemistry. 2001; 40:8842–8851. [PubMed: 11467945]

Demeure O, Lecerf F, Duby C, Desert C, Ducheix S, Guillou H, Lagarrigue S. Regulation of LPCAT3 by LXR. Gene. 2011; 470:7–11. [PubMed: 20837115]

Erbay E, Babaev VR, Mayers JR, Makowski L, Charles KN, Snitow ME, Fazio S, Wiest MM, Watkins SM, Linton MF, Hotamisligil GS. Reducing endoplasmic reticulum stress through a macrophage lipid chaperone alleviates atherosclerosis. Nature medicine. 2009; 15:1383–1391.

Faloia E, Garrapa GG, Martarelli D, Camilloni MA, Lucarelli G, Staffolani R, Mantero F, Curatola G, Mazzanti L. Physicochemical and functional modifications induced by obesity on human erythrocyte membranes. European journal of clinical investigation. 1999; 29:432–437. [PubMed: 10354200]

Feng B, Yao PM, Li Y, Devlin CM, Zhang D, Harding HP, Sweeney M, Rong JX, Kuriakose G, Fisher EA, Marks AR, Ron D, Tabas I. The endoplasmic reticulum is the site of cholesterol-induced cytotoxicity in macrophages. Nature cell biology. 2003; 5:781–792.

Fu S, Yang L, Li P, Hofmann O, Dicker L, Hide W, Lin X, Watkins SM, Ivanov AR, Hotamisligil GS. Aberrant lipid metabolism disrupts calcium homeostasis causing liver endoplasmic reticulum stress in obesity. Nature. 2011; 473:528–531. [PubMed: 21532591]

Funk CD. Prostaglandins and leukotrienes: advances in eicosanoid biology. Science. 2001; 294:1871–1875. [PubMed: 11729303]

Hishikawa D, Shindou H, Kobayashi S, Nakanishi H, Taguchi R, Shimizu T. Discovery of a lysophospholipid acyltransferase family essential for membrane asymmetry and diversity. Proceedings of the National Academy of Sciences of the United States of America. 2008; 105:2830–2835. [PubMed: 18287005]

Holzer RG, Park EJ, Li N, Tran H, Chen M, Choi C, Solinas G, Karin M. Saturated fatty acids induce c-Src clustering within membrane subdomains, leading to JNK activation. Cell. 2011; 147:173–184. [PubMed: 21962514]

Hong C, Tontonoz P. Coordination of inflammation and metabolism by PPAR and LXR nuclear receptors. Current opinion in genetics & development. 2008; 18:461–467. [PubMed: 18782619]

Ishibashi M, Varin A, Filomenko R, Lopez T, Athias A, Gambert P, Blache D, Thomas C, Gautier T, Lagrost L, Masson D. Liver x receptor regulates arachidonic acid distribution and eicosanoid release in human macrophages: a key role for lysophosphatidylcholine acyltransferase 3. Arteriosclerosis, thrombosis, and vascular biology. 2013; 33:1171–1179.

Kabarowski JH. G2A and LPC: regulatory functions in immunity. Prostaglandins & other lipid mediators. 2009; 89:73–81. [PubMed: 19383550]

Lands WE. Metabolism of glycerolipides; a comparison of lecithin and triglyceride synthesis. The Journal of biological chemistry. 1958; 231:883–888. [PubMed: 13539023]

Li, L.; Medina, JC.; Hasegawa, H.; Cutler, ST.; Liu, J.; Zhu, L.; Shan, B.; Lustig, K. Preparation of bis(trifluoromethyl)hydroxymethylbenzenesulfonamides, -ureas, and -carbamates as liver X receptor modulators. PCT Int Appl. WO 2000/054759 A2 20000921. 2000.

Li Y, Ge M, Ciani L, Kuriakose G, Westover EJ, Dura M, Covey DF, Freed JH, Maxfield FR, Lytton J, Tabas I. Enrichment of endoplasmic reticulum with cholesterol inhibits sarcoplasmic-endoplasmic reticulum calcium ATPase-2b activity in parallel with increased order of membrane lipids: implications for depletion of endoplasmic reticulum calcium stores and apoptosis in cholesterol-loaded macrophages. The Journal of biological chemistry. 2004; 279:37030–37039. [PubMed: 15215242]

Li Z, Ding T, Pan X, Li Y, Li R, Sanders PE, Kuo MS, Hussain MM, Cao G, Jiang XC. Lysophosphatidylcholine acyltransferase 3 knockdown-mediated liver lysophosphatidylcholine accumulation promotes very low density lipoprotein production by enhancing microsomal triglyceride transfer protein expression. The Journal of biological chemistry. 2012; 287:20122–20131. [PubMed: 22511767]

Miyazaki M, Kim YC, Gray-Keller MP, Attie AD, Ntambi JM. The biosynthesis of hepatic cholesterol esters and triglycerides is impaired in mice with a disruption of the gene for stearoyl-CoA desaturase 1. The Journal of biological chemistry. 2000; 275:30132–30138. [PubMed: 10899171]

Ozcan U, Cao Q, Yilmaz E, Lee AH, Iwakoshi NN, Ozdelen E, Tuncman G, Gorgun C, Glimcher LH, Hotamisligil GS. Endoplasmic reticulum stress links obesity, insulin action, and type 2 diabetes. Science. 2004; 306:457–461. [PubMed: 15486293]

Repa JJ, Liang G, Ou J, Bashmakov Y, Lobaccaro JM, Shimomura I, Shan B, Brown MS, Goldstein JL, Mangelsdorf DJ. Regulation of mouse sterol regulatory element-binding protein-1c gene (SREBP-1c) by oxysterol receptors, LXRalpha and LXRbeta. Genes & development. 2000; 14:2819–2830. [PubMed: 11090130]

Solinas G, Vilcu C, Neels JG, Bandyopadhyay GK, Luo JL, Naugler W, Grivennikov S, Wynshaw-Boris A, Scadeng M, Olefsky JM, Karin M. JNK1 in hematopoietically derived cells contributes to diet-induced inflammation and insulin resistance without affecting obesity. Cell metabolism. 2007; 6:386–397. [PubMed: 17983584]

Spector AA, Yorek MA. Membrane lipid composition and cellular function. Journal of lipid research. 1985; 26:1015–1035. [PubMed: 3906008]

Tuncman G, Hirosumi J, Solinas G, Chang L, Karin M, Hotamisligil GS. Functional in vivo interactions between JNK1 and JNK2 isoforms in obesity and insulin resistance. Proceedings of the National Academy of Sciences. 2006; 103:10741–10746.

Venkateswaran A, Laffitte BA, Joseph SB, Mak PA, Wilpitz DC, Edwards PA, Tontonoz P. Control of cellular cholesterol efflux by the nuclear oxysterol receptor LXR alpha. Proceedings of the National Academy of Sciences of the United States of America. 2000; 97:12097–12102. [PubMed: 11035776]

Volmer R, van der Ploeg K, Ron D. Membrane lipid saturation activates endoplasmic reticulum unfolded protein response transducers through their transmembrane domains. Proceedings of the National Academy of Sciences of the United States of America. 2013; 110:4628–4633. [PubMed: 23487760]

Wang S, Chen Z, Lam V, Han J, Hassler J, Finck BN, Davidson NO, Kaufman RJ. IRE1alpha-XBP1s induces PDI expression to increase MTP activity for hepatic VLDL assembly and lipid homeostasis. Cell metabolism. 2012; 16:473–486. [PubMed: 23040069]

Wellen KE, Hotamisligil GS. Inflammation, stress, and diabetes. The Journal of clinical investigation. 2005; 115:1111–1119. [PubMed: 15864338]

Zelcer N, Khanlou N, Clare R, Jiang Q, Reed-Geaghan EG, Landreth GE, Vinters HV, Tontonoz P. Attenuation of neuroinflammation and Alzheimer's disease pathology by liver x receptors. Proceedings of the National Academy of Sciences of the United States of America. 2007; 104:10601–10606. [PubMed: 17563384]

Zhao Y, Chen YQ, Bonacci TM, Bredt DS, Li S, Bensch WR, Moller DE, Kowala M, Konrad RJ, Cao G. Identification and characterization of a major liver lysophosphatidylcholine acyltransferase. The Journal of biological chemistry. 2008; 283:8258–8265. [PubMed: 18195019]
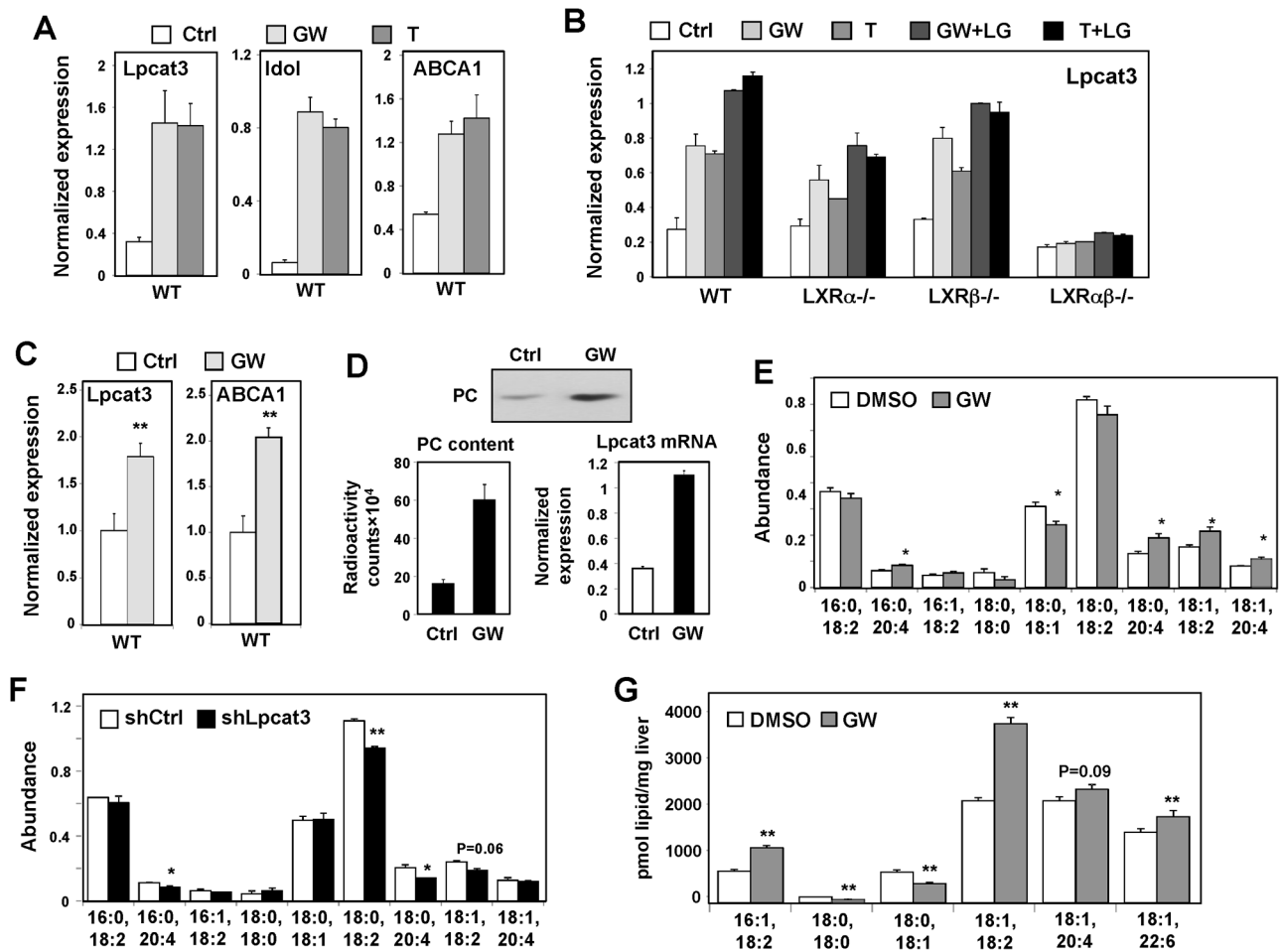
Rong Highlights

Induction of Lpcat3 expression by LXRs promotes phospholipid remodeling

LXR-Lpct3 activation drives unsaturated fatty acid incorporation into phospholipids

Lpcat3 activity in liver modulates lipid-induced ER stress and inflammation

Lpcat3 affects inflammation through regulation of membrane c-Src activity

Figure 1. LXRs regulate Lpcat3 expression and activity

(A) Primary mouse hepatocytes were treated with GW3965 (GW, 1 μM) and T0901317 (T, 1 μM) overnight. Gene expression in this and all subsequent figures was analyzed by real-time PCR. Results are representative of three independent experiments. Values are means ± SD.

(B) LXR-dependent regulation of Lpcat3 in primary mouse hepatocytes after overnight treatment with GW (1μM) or T (1 μM), and/or the RXR ligand LG268 (LG, 50 nM). Results are representative of two independent experiments. Values are means ± SD.

(C) Induction of Lpcat3 mRNA expression in livers of mice treated with 40 mg/kg/day GW3956 by oral gavage for 3 days (N=5 per group). Values are means ± SEM.

(D) Stable Raw 264.7-LXRα cells were treated with the LXR agonist GW (1 μM). Microsomal Lpcat3 activity was measured by radiolabeled acyltransferase assay. Thin-layer chromatogram is shown (upper panel); radioactivity in excised bands was quantified by scintillation counter (low left). Induction of Lpcat3 mRNA was measured by real-time PCR (lower right). Results are representative of two independent experiments. Values are means ± SD.

(E) ESI-MS/MS analysis of the abundance of PC species in Raw 264.6 cells treated with GW3965 (1 μM) for 48 h. N=3 per group. Values are means ± SEM.

(F) ESI-MS/MS analysis of the abundance of PC species in Raw 264.6 cells stably expressing shRNA targeting Lpcat3 (shLpcat3) or LacZ (shCtrl). N=3 per group. Values are means ± SEM.

(G) ESI-MS/MS analysis of the abundance of PC species in livers from C57BL/6 mice treated with 20 mg/kg GW3965 by oral gavage, 2 doses/day for 2 days (N=5 per group). Values are means ± SEM.

Statistical analysis was performed using student's t-test (C, E, F and G). *p < 0.05; **p < 0.01. See also Figure S1.
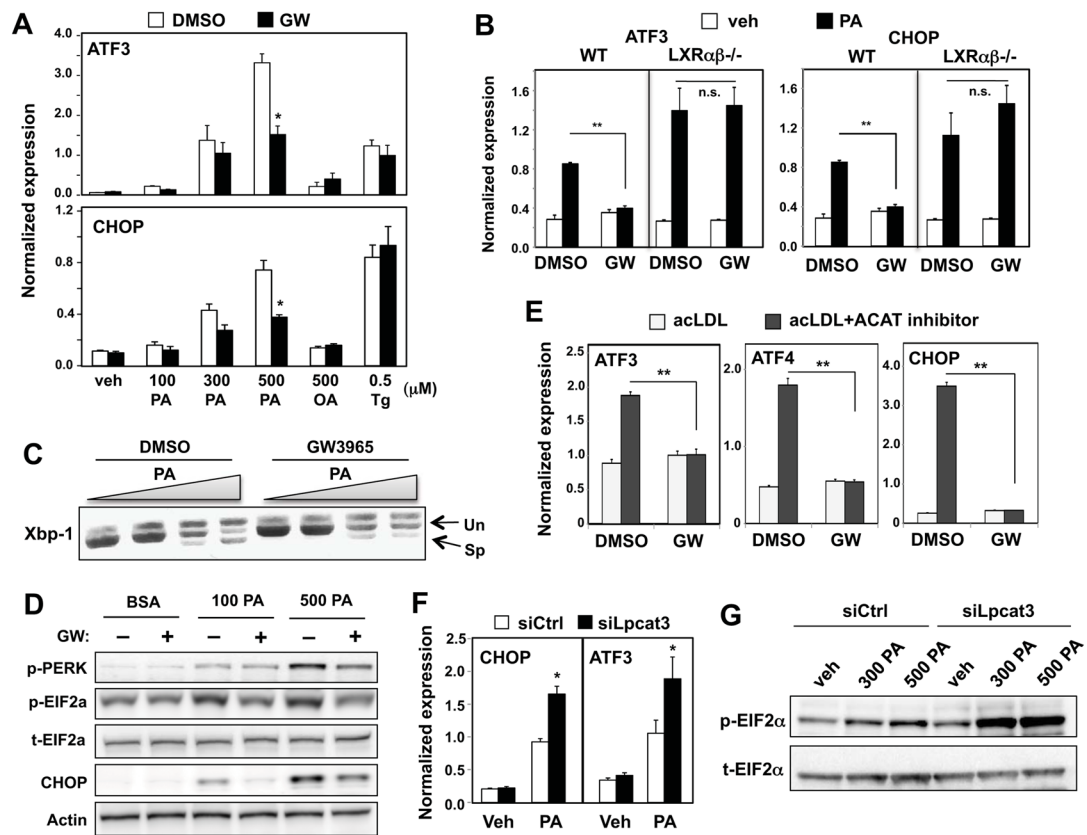
Figure 2. LXRs and Lpcat3 attenuate lipid-induced ER stress
(A) Hep3B cells were pretreated with GW3965 (1 μM) for 24 h, followed by stimulation with BSA-conjugated palmitic acid (PA), BSA-conjugated oleic acid (OA) or thapsigargin (Tg) at the indicated concentration for 6 h. Induction of CHOP and ATF3 mRNA was analyzed by real-time PCR. Values are means ± SD.
(B) Primary hepatocytes from wild-type and *LXRαβ−/−* mice were pre-treated with GW3965 (1 μM) for 24 h and then stimulated with 500 μM BSA-conjugated PA. Values are means ± SD.
(C) Hep3B cells were pretreated with GW3965 (GW) 1 μM for 24 h, followed by stimulation with BSA-conjugated PA. Induction of Xbp-1 splicing was analyzed by PCR and gel electrophoresis.
(D) Hep3B cells were pre-treated with GW3965 (1 μM) for 24 h and stimulated with BSA-conjugated PA at the indicated concentrations. Activation of UPR signaling was analyzed by Immunoblotting.
(E) Concanavalin A-elicited peritoneal macrophages were treated with GW3965 (1 μM) and loaded with cholesterol by incubating with acetylated-LDL (ac-LDL) alone or acylated-LDL and ACAT inhibitor to induce ER stress. Values are means ± SD.
(F) Hep3B cells were transfected with siRNA targeting Lpcat3 (siLpcat3) or scramble (siCtrl) for 48 h, followed by stimulation with BSA-conjugated PA. Values are means ± SD.
(G) Hep3B cells were transfected as in F. Phosphorylation of eIF2α was analyzed by immunoblot. t-EIF2α, total EIF2α; p-EIF2α, phospho-EIF2α.
Statistical analysis was by two-way ANOVA with Bonferroni post hoc tests (A, B, E and F): *p < 0.05; **p < 0.01; n.s., not significant. See also Figure S2.
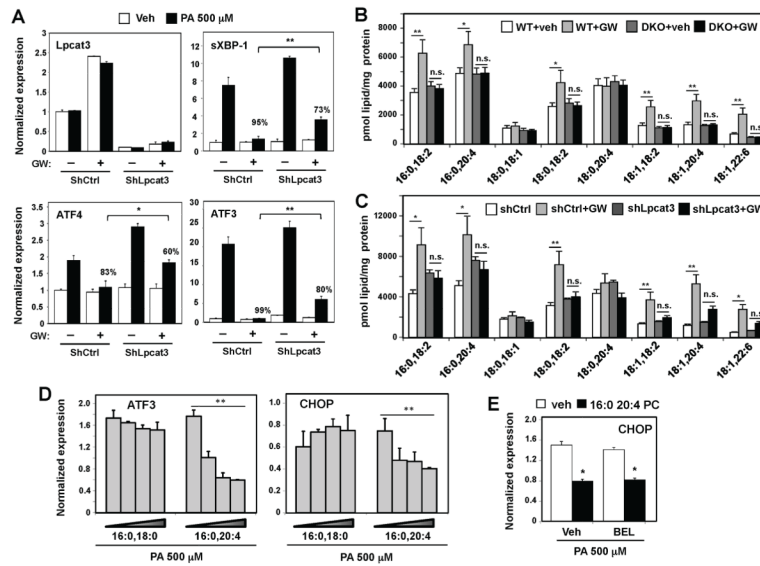
Figure 3. Lpcat3 contributes to LXR-dependent PL remodeling and ER stress reduction

(A) Primary mouse hepatocytes were transfected with adenoviral shRNA targeting Lpcat3 (shLpcat3) or control (shCtrl) for 48 h, with GW3965 (1 μM) treatment for the last 24 h, followed by stimulation with 500 μM BSA-conjugated PA. Gene expression was analyzed by real-time PCR. The % repression of PA-induced gene expression by GW is indicated for control versus Lpcat3 knockdown. Values are means ± SEM.

(B) ESI-MS/MS analysis of the abundance of PC species in primary hepatocytes from wild-type or $LXR\alpha\beta^{-/-}$ (DKO) mice treated with GW3965 (1 μM) for 48 h. N=3 per group. Values are means ± SEM.

(C) ESI-MS/MS analysis of the abundance of PC species in wild-type primary hepatocytes transfected with adenoviral shRNA targeting Lpcat3 (shLpcat3) or control (shCtrl) for 48 h and treated with GW3965 (1 μM) for the last 24 h. N=3 per group. Values are means ± SEM.

(D) Hep3B cells were treated with increasing concentrations of liposomes composed of different species of PC, followed by stimulation with BSA-conjugated PA at 500 μM. Values are means ± SD.

(E) Hep3B cells were treated with vehicle or 1 μM bromoenol lactone (BEL) and then incubated with liposomes made with 16:0 20:4 PC or vehicle (veh). 500 μM BSA-conjugated PA was used to stimulated ER stress. Values are means ± SD.

Statistical analysis was by student's t-test (A, over the % repression in shCtrl), one-way ANOVA with Bonferroni post hoc tests (D) or two-way ANOVA with Bonferroni post hoc tests (B, C and E): *$p < 0.05$; **$p < 0.01$; N.S., not significant.
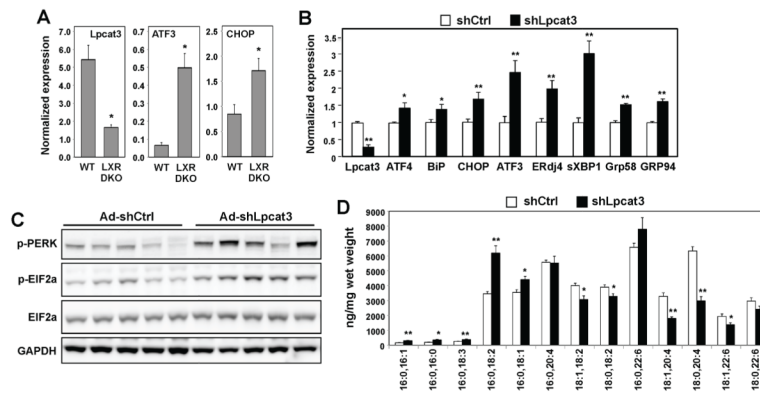
**Figure 4. Inhibition of the LXR-Lpcat3 pathway increases ER stress *in vivo***
(A) Wild-type and *Lxrαβ−/−* (DKO) mice were fed a western diet for 12 weeks. Liver gene expression was analyzed by real-time PCR. N=4–5 per group. Values are means ± SEM.
(B) *ob/ob* mice were transduced with adenoviral-expressed shRNA targeting Lpcat3 (shLpcat3) or control (shCtrl) for 7 days. UPR signaling in livers was analyzed by real-time PCR on day 7, normalized to Gapdh and shown as fold change over shCtrl. N=6 per group. Values are means ± SEM.
(C) Immunoblot analysis of protein expression in livers of *ob/ob* mice transduced with adenoviral shCtrl or shLpcat3 for 7 days.
(D) ESI-MS/MS analysis of liver PC species from *ob/ob* mice transduced with adenoviral shCtrl or shLpcat3 for 7 days. N=6 per group. Values are means ± SEM.
Statistical analysis was performed using student's t-test. *p < 0.05; **p < 0.01. See also Figure S3.
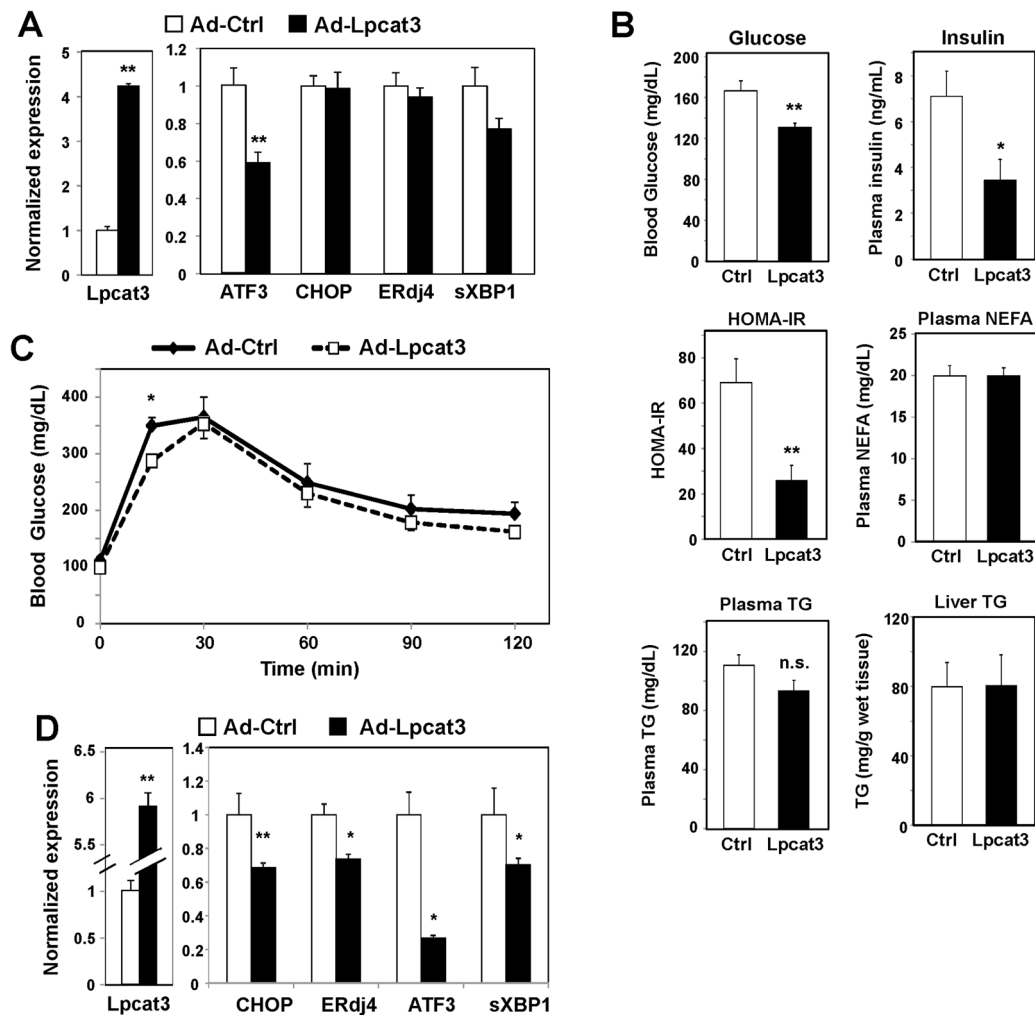
Figure 5. Expression of Lpcat3 in mouse liver affects metabolism and reduces ER stress

(A) *ob/ob* mice were transduced with adenovirus expressing Lpcat3 (Ad-Lpcat3) or control EGFP (Ad-Ctrl) for 7 days. Liver gene expression was determined by real-time PCR, normalized to 36B4, and presented as fold change over Ad-Ctrl. N=6 per group. Values are means ± SEM.

(B) Metabolic parameters in *ob/ob* mice transduced with Ad-Ctrl or Ad-Lpcat3 for 7 days. N=6 per group. Values are means ± SEM.

(C) Glucose tolerance test performed on *ob/ob* mice transduced with Ad-Ctrl or Ad-Lpcat3 4 d after infection. N=6 per group. Values are means ± SEM.

(D) *db/db* mice were transduced with Ad-Ctrl or Ad-Lpcat3 for 7 d. Gene expression was determined by real-time PCR, normalized to 36B4 and shown as fold change over Ad-Ctrl. N=5 per group. Values are means ± SEM.

Statistical analysis was performed using student's t-test compared to control. *p < 0.05; **p < 0.01.
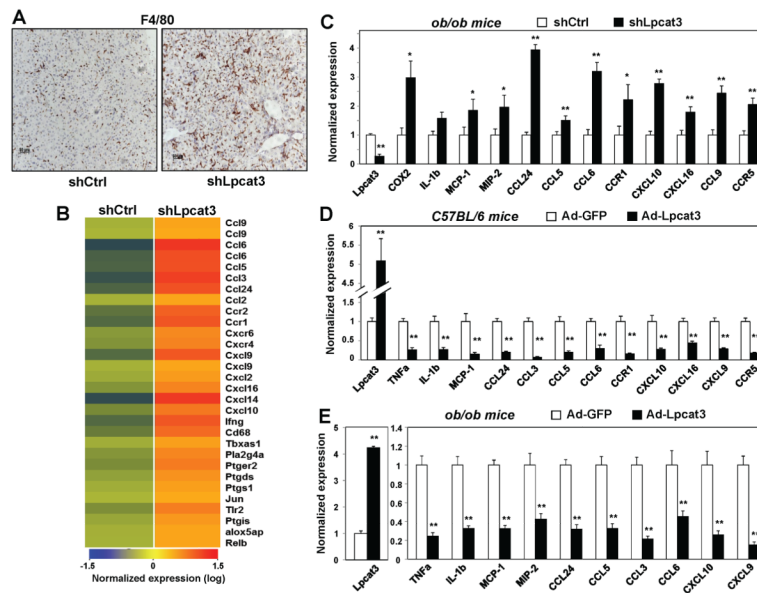
Figure 6. Lpcat3 activity modulates hepatic inflammation *in vivo*

(A) Immunostaining with F4/80 antibody of liver sections from C57BL/6 mice transduced with adenoviral-expressed shRNA targeting Lpcat3 (shLpcat3) or control (shCtrl) for 8 d.

(B) C57BL/6 mice were transduced with adenovirus-expressed shLpcat3 or shCtrl. Gene expression in livers was analyzed by Affymetrix arrays after 8 d. Select inflammatory genes are presented by heatmap. N=5 per group.

(C) Gene expression of livers from *ob/ob* mice transduced with shLpcat3 or shCtrl for 7 d. Results were normalized to 36B4 and are presented as fold change over shCtrl. N=6 per group. Values are means ± SEM.

(D) Gene expression of livers from C57BL/6 mice transduced with adenoviral-expressed Lpcat3 (Ad-Lpcat3) or control EGFP (Ad-GFP) for 9 d. N=6 per group. Results were normalized to 36B4 and are presented as fold change over Ad-GFP. Values are means ± SEM.

(E) Gene expression of livers from *ob/ob* mice transduced with Ad-Lpcat3 or Ad-GFP for 7 days. N=6 per group. Results were normalized to 36B4 and are presented as fold change over Ad-GFP. Values are means ± SEM. Statistical analysis was by student's t-test. *p < 0.05; **p < 0.01. See also Figure S4.
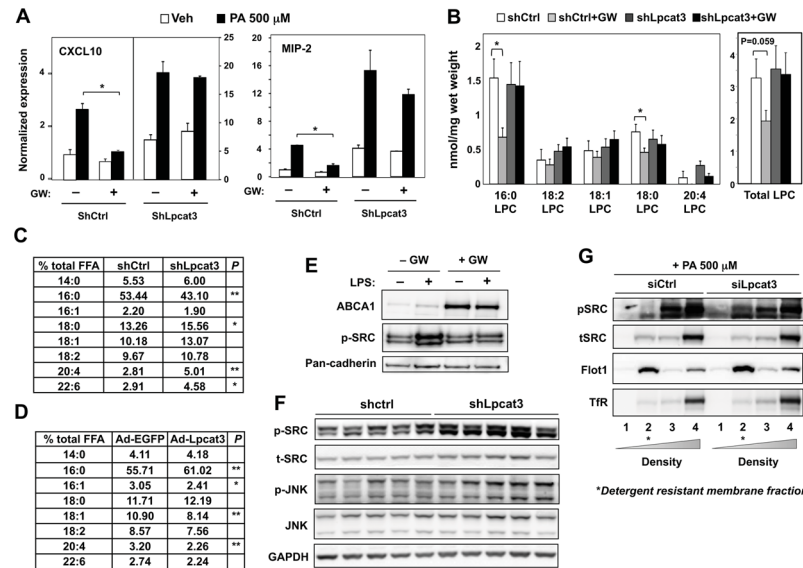
Figure 7. Lpcat3 activity controls lipid mediator availability and c-Src activation
(A) Primary hepatocytes were transduced with adenoviral-expressed shLpcat3 or shCtrl at MOI 10 for 60 h and treated with vehicle or GW3965 for 24 h, followed by PA stimulation. Gene expression was analyzed by real-time PCR, normalized to 36B4 and shown as fold change over veh+DMSO+shctrl. Values are means ± SD.
(B) ESI-MS/MS analysis of lysophosphatidylcholine species in the livers from C57BL/6 mice transduced with shLpcat3 or shCtrl for 8 d, and gavaged with GW3965 at 40 mg/kg body weight once per day on day 6, 7 and 8. N=5 per group. Values are means ± SEM.
(C) GC-MS analysis of free fatty acid species in the livers from C57BL/6 mice transduced with shLpcat3 or shCtrl for 8 d. Results are presented as % of total free fatty acid.
(D) GC-MS analysis of free fatty acid species in the livers from C57BL/6 mice transduced with Ad-Lpcat3 or Ad-EGFP. N=6 per group. Results are presented as % of total free fatty acid.
(E) Primary mouse macrophages were treated with GW3965 (1 μM) and stimulated with 10 ng/ml LPS. Cellular membranes were isolated by ultracentrifugation and analyzed by immunoblotting.
(F) Immunoblot analysis of livers from *ob/ob* mice transduced with adenoviral shLpcat3 or shCtrl for 7 d.
(G) Hep3B cells were transfected with adenoviral shLpcat3 or shCtrl for 48 h, followed by stimulation with 500 μM BSA-conjugated PA. Detergent-resistant membrane were isolated by gradient centrifugation and analyzed by immunoblotting.
Statistical analysis was by student's t-test (A, D and E) or two-way ANOVA with Bonferroni post hoc tests (B). For (C), student's t-test was performed between vehicle and GW treatment in each subgroup. *p < 0.05; **p < 0.01. See also Figure S5.